



## CHAPTER IV

### EFFECTS OF MARL ON THERMAL AND MECHANICAL PROPERTIES OF POLYBENZOXAZINE COMPOSITES: SYNTHESIS AND CHARACTERIZATION

#### 4.1 ABSTRACT

Polybenzoxazine (PBZ) exhibits high thermal stability and stiffness but low flexural strain and toughness. Herein, polybenzoxazine precursors have been synthesized from aliphatic diamine, bisphenol-A, and paraformaldehyde to obtain a high molecular weight benzoxazine precursor. The synthesized polybenzoxazine was blended with marl to improve the mechanical properties. In this study, a quasi-solventless approach is used, which enables a faster reaction time than the other systems that have been reported, while a comparable yield (88%) is obtained. The results from Fourier transform infrared (FTIR) of the polybenzoxazine spectrum; tri-substituted benzene rings at  $1498\text{ cm}^{-1}$  and out-of-plane bending vibrations of C-H of oxazine ring at  $929\text{ cm}^{-1}$ , confirmed the functional groups of the precursors. Thermal properties of the composite were investigated by differential scanning calorimetry (DSC) and thermogravimetry (TGA), which exhibited the lower curing temperature and the higher thermal stability after increasing the marl contents on the polybenzoxazine-marl composite. Due to the aggregation between marl and polybenzoxazine matrix, revealed by SEM, (3-aminopropyl)trimethoxysilane and stearic acid were chosen as the surface modifying agents for better adhesion, which brings about the better mechanical properties in flexural and impact strength.

**Keywords:** Marl, Polybenzoxazine, Composite

#### 4.2 INTRODUCTION

Polybenzoxazine is a newly developed, additionally cured phenolic resin, which not only provides the good characteristics found in traditional phenolic resin but also has some new excellent thermal and flame retardance properties, as well as

good dimensional stability. However, there are some disadvantages for the cured polybenzoxazine, namely its brittleness and relatively high curing temperature. Benzoxazine (BZ) monomers are typically synthesized by employing solution method or solventless method (melt-state process) through the Mannich condensation of phenol, formaldehyde, and amine. Because of the brittleness, much of the published benzoxazine research has targeted the improvement of the toughness of these materials. Ishida *et al.* [2,6–7] tried to reduce the brittleness of polybenzoxazine by blending it with poly( $\epsilon$ -caprolactone) and developing a new class of difunctional or multifunctional benzoxazine monomers by using bisphenol-A and diamine to conquer the limits of the product resulting from the mono-functional benzoxazines, which give only oligomeric structure. Takeichi *et al.* [15] synthesized high molecular weight polybenzoxazine precursors, which improved the toughness of the crosslink polybenzoxazine film.

Marl, which is known in Thai as “din-so-pong” or white soil, contains more than 80% calcium carbonate; it can be used as a cool powder for anti-sweating, anti-infection, and skin disease reduction. Because of its advantages, marl, which is similar to calcium carbonate or clay, was chosen to use as a filler to improve the mechanical properties, which can lower the price of the product at the same time. Nevertheless, its polar nature often requires surface treatment before incorporation into a non-polar plastic matrix in order to modify the filler–polymer interactions, and to facilitate the dispersion in the polymer matrix. To improve the compatibility, resulting in high mechanical properties of the composites, different coupling agents, for example silanes and titanates, can be applied [8, 3, 10]. Moreover, much cheaper nonreactive coupling agents, such as fatty acids or stearic acid, also can be successfully used in calcium carbonate–polymer composites (Wang *et al.* [17]).

In this work, a newly developed quasi-solventless approach is used for the synthesis of polybenzoxazine precursors with a faster reaction time using 1,6-diaminohexane, bisphenol-A, and paraformaldehyde. The characterization of the precursors covers functional group analysis, chemical structure, and thermal and mechanical properties. Afterwards, the synthesized polybenzoxazine precursor was blended with marl—din-so-pong—at various ratios to optimize the mechanical properties of the composites.

### 4.3 EXPERIMENTAL

#### Materials

Bisphenol-A (97% purity) was supplied from Sigma Aldrich Chemical. Paraformaldehyde (98.7% purity) was supplied from Merck. 1,6-Diaminohexane (99% purity) was supplied from Fluka. The marl, or marly limestone, used is a product from Lopburi Province, Thailand. The modifying agents, stearic acid ( $\text{CH}_3(\text{CH}_2)_{16}\text{COOH}$ ) and silane coupling agent—(3-aminopropyl)trimethoxysilane,  $\text{NH}_2(\text{CH}_2)_3\text{Si}(\text{OCH}_3)_3$ —were purchased from Sigma Aldrich Chemical.

1,4-dioxane (AR grade) was supplied from Lab Scan Co., Ltd. Tetrahydrofuran (THF, HPLC grade) was purchased from Burdick&Jackson supplier (B&J). Methyl and Ethyl alcohol were purchased from Italmar. All chemicals are used without further purification.

#### Synthesis of Aliphatic Diamine Based on a Polybenzoxazine Precursor via the Quasi-Solventless Method

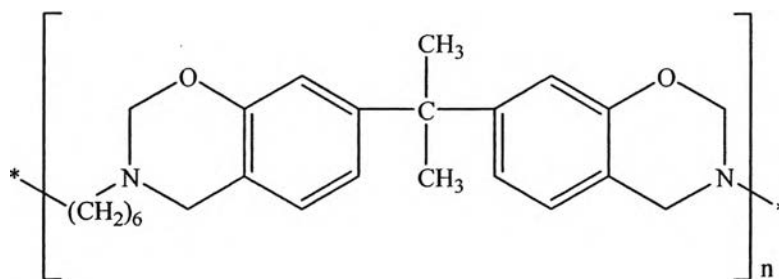


**Figure 4.1** Schematic structure of the synthesized polybenzoxazine.

The polybenzoxazine precursor (shown in Figure 4.1) was prepared by reacting bisphenol-A (6 mmol) with a paraformaldehyde solution (24 mmol) in 1,4-dioxane at  $10^\circ\text{C}$ . The mixture was stirred continuously before a solution of 1,6-diaminohexane (6 mmol) in 1,4-dioxane was slowly added, and then it was stirred continuously until the solution formed a gel. The reaction temperature was then raised to  $80\text{--}90^\circ\text{C}$ ; the mixture was continuously stirred for 1 h until a clear homoge-

neous yellow viscous liquid was obtained. The chemical structure of the precursors was confirmed by FTIR and  $^1\text{H NMR}$ .

### **Preparation of Polybenzoxazine–Marl Composites**

The marl was pulverized and sieved through a 325-hole mesh. The obtained marl was dissolved in 1,4-dioxane and stirred by a homogenizer at 8000 rpm for 30 min. Various concentrations (10–50 wt%) of the composites can be prepared by adding homogenized marl solution to the synthesized polybenzoxazine precursor, and a homogeneous solution was obtained after thorough mixing. The mixture was step-cured in a compression molding (Wabash, model V50H-18-CX) at a force of 20 ton to be a thin sheet with 3 mm thickness. The polymerization temperature profile for compression molding process of polybenzoxazine and composites were obtained at 80, 100, 120, 150, 180, and 210°C. The composite sheets were cut into the specific sizes and were characterized by FTIR, DSC, TGA, SEM, DMA, flexural, and tensile testing.

### **Surface Modification of a Marl Filler**

Surface modification of marl with amino silane was carried out in solution. An aqueous ethyl alcohol solution was prepared, and the silane coupling agent (1 wt% filler) was added to the solution, which was then mixed by a stirrer for 15 min. Afterwards, the sieved marl was added to the silane/water mixture and stirred for 2 h while the filler treated with stearic acid (1 wt% filler) was suspended in approximately 360 ml of toluene per 100 g filler. The solution was stirred continuously. When the set reaction time elapsed, the solution was dried under vacuum. The treated marl was pulverized and sieved again before the preparation of the polybenzoxazine–marl composites. The chemical analysis and morphology were obtained with FTIR and SEM, respectively.

### **Characterization**

The presence of functional groups of polymers was determined by using an FTIR Nicolet Nexus 670 spectrometer in the frequency range of 4000–400  $\text{cm}^{-1}$  with 32 scans at a resolution of 4  $\text{cm}^{-1}$  by using a KBr pellet technique. Proton Nuclear

Magnetic Resonance (NMR) spectra were recorded on a Varian Inova 500 NMR working at 500 MHz. The morphology was studied by scanning electron microscopy (JEOL JSM-5410) at 15 kV. The thermal stability was investigated by differential scanning calorimetry (DSC) using a Perkin-Elmer DSC 7 instrument by heating the samples from 50–400°C at a rate of 10°C/min under a N<sub>2</sub> atmosphere with a flow rate of 20 ml/min and thermal decomposition temperatures were observed with a Mettler TGA (Thermogravimetric analysis) instrument. The samples were heated from 50–850°C at a heating rate of 10°C/min under a N<sub>2</sub> flow of 50 mL/min. Dynamic mechanical analysis (DMA) were obtained with a dynamic-mechanical analyzer NETZSCH DMA 242 instrument. The specimens with dimensions of approximately 60×10×3 mm<sup>3</sup> were tested in a rectangular torsion fixture. A sinusoidal shear strain of 0.1% was applied at a frequency 1 Hz during each temperature sweep experiment. Linearity of the chosen shear strain was verified by a strain sweep prior to each experiment. Measurement were collected every 2°C as the samples were heated at a rate of approximately 3°C/min from -100°C to well above the glass transition of each material.

Flexural testing was performed using an Instron/4206 Universal Testing Machine (UTM). The flexural specimens were prepared according to ASTM D790M. The UTM was fitted with a 5 kN static load cell and a standard 3-point bending fixture. Flexural test specimens, with dimensions of 60×10×3 mm<sup>3</sup>, were tested for each material using the Series IX control and analysis software. The samples were flexed until breakage at a rate 1.28 mm/min using a support span of 48 mm. Flexural strain was calculated based on crosshead movement. The flexural stress, modulus, and strain were reported from at least five average values. The impact testing was performed by cutting sheets of sample into the specimen shape following the ASTM D256 (notched IZOD type) with dimensions of 64×12.7×3.2 mm<sup>3</sup>, then the impact strength was tested by the ZWICK impact testing machine with the pendulum load of 2.7 J. The impact strength was reported from at least five average values.

Gel Permeation Chromatography (GPC) Shimadzu Model was carried out in THF solvent as the mobile phase using Waters Styragel THF Column and RID-

10A detector. The THF solvent was filtrated with MN 615 Ø 155 mm filter paper under the vacuum. The crude polymers were dissolved in THF at the concentration 0.5 wt% and filtrated with 0.45 mm diameter of cellulose acetate filter before injecting into the column. The conditions of this machine were 40°C column temperature, 1 ml/min flow rate, and 30 min run time. Molecular weight and molecular weight distribution of PBZ were calculated in reference to a polystyrene calibration.

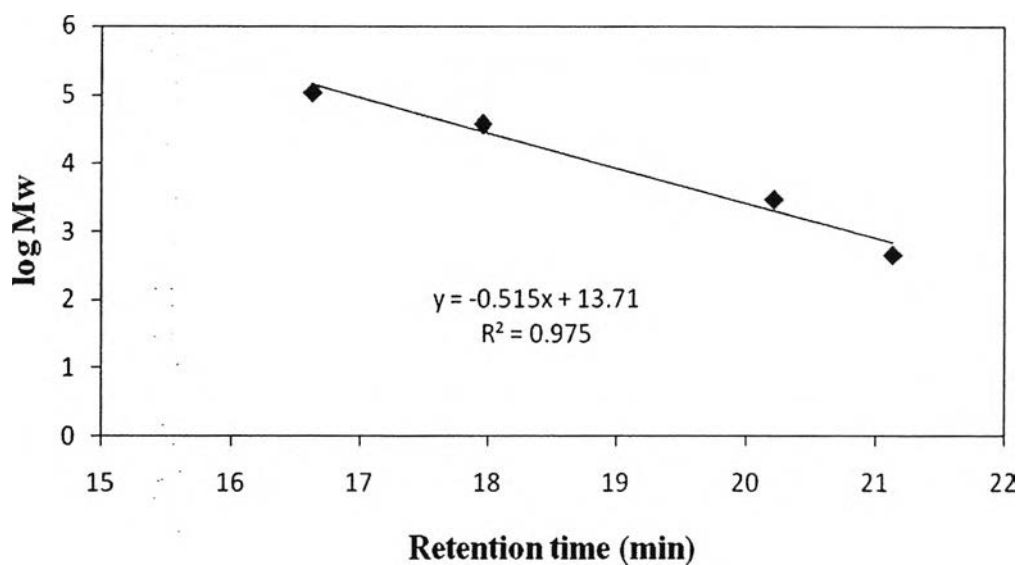


**Figure 4.2** The polystyrene calibration for the calculation of molecular weight.

## 4.4 RESULTS AND DISCUSSION

### 4.4.1 Preparation and Characterization of the Polybenzoxazine Precursors

#### 4.4.1.1 Preparation of Polybenzoxazine Precursors

The synthesis of precursors is based on the Mannich reaction of bisphenol-A, 1,6-Diaminohexane, and paraformaldehyde at the molar ratio of 1:1:4. The reaction conditions of the precursor synthesis were examined first. Takeichi *et al.*, 2005 suggested that the solventless method was difficult to apply due to the insoluble bulky solid was obtained after heating the mixture of benzoxazine reactants for half an hour. However, they were successful in the synthesis the precursor with the solvent method by refluxing the mixture in chloroform but it took a long reaction time (6 h), and large amount of gel was formed resulted to decrease the yield. Therefore, a quasi-solventless approach was developed with the similar idea of increase reactants concentration to the solventless method. Followed from the Rate equation or rate law:

$$R = k(T) [A]^{n'} [B]^{m'} \quad (1)$$

For a chemical reaction  $n A + m B \rightarrow C + D$ , the rate equation or rate law is a mathematical expression used in chemical kinetics to link the rate of a reaction to the concentration of each reactant, [A] and [B]. The exponents  $n'$  and  $m'$  are called reaction orders and depend on the reaction mechanism. In this equation  $k(T)$  is the reaction rate coefficient or rate constant, although it is not really a constant, because it includes all the parameters that affect reaction rate, except for concentration. Each reaction rate coefficient,  $k$ , has a temperature dependency, which is usually given by the Arrhenius equation:

$$k = A e^{-E_a/RT} \quad (2)$$

$E_a$  is the activation energy and  $R$  is the gas constant. Since at temperature  $T$  the molecules have energies given by a Boltzmann distribution, one can expect the number of collisions with energy greater than  $E_a$  to be proportional to  $e^{-E_a/RT}$ .  $A$  is the pre-exponential factor or frequency factor. The values for  $A$  and  $E_a$  are dependent on the reaction.

When comparing the quasi-solventless approach with the traditional solvent method, the quasi-solventless approach used the lower amount of solvent and it was evaporated out during the reaction process, which means the higher concentration of reactants. Therefore with this new method the reaction time is less. The solution of bisphenol-A, paraformaldehyde, and 1,6-diaminohexane in 1,4-dioxane solvent were mixed together at the cooling temperature because lower temperature will decrease reaction rate coefficient,  $k$ , resulted in a controllable reaction. After stirring for a while, the mixture will form gel. The formed gel was stirred and reduced to become a clear solution again at 90°C. After alcohol purification, the yield of crude product was in the range of 88–91%.

Molecular weight and molecular weight distribution of the resulting precursor was estimated from gel permeation chromatography (GPC). GPC was carried out in THF solvent using Waters Styragel THF Column with a refractometer index detector. The resulted GPC curve is shown in Figure 4.3, which molecular weight and molecular weight distribution of these polymers were calculated in reference to a following polystyrene calibration:

$$\text{Log } M = -0.51520169T_r + 13.71764303 \quad (3)$$

$$\text{With dispersion} = 0.1468805$$

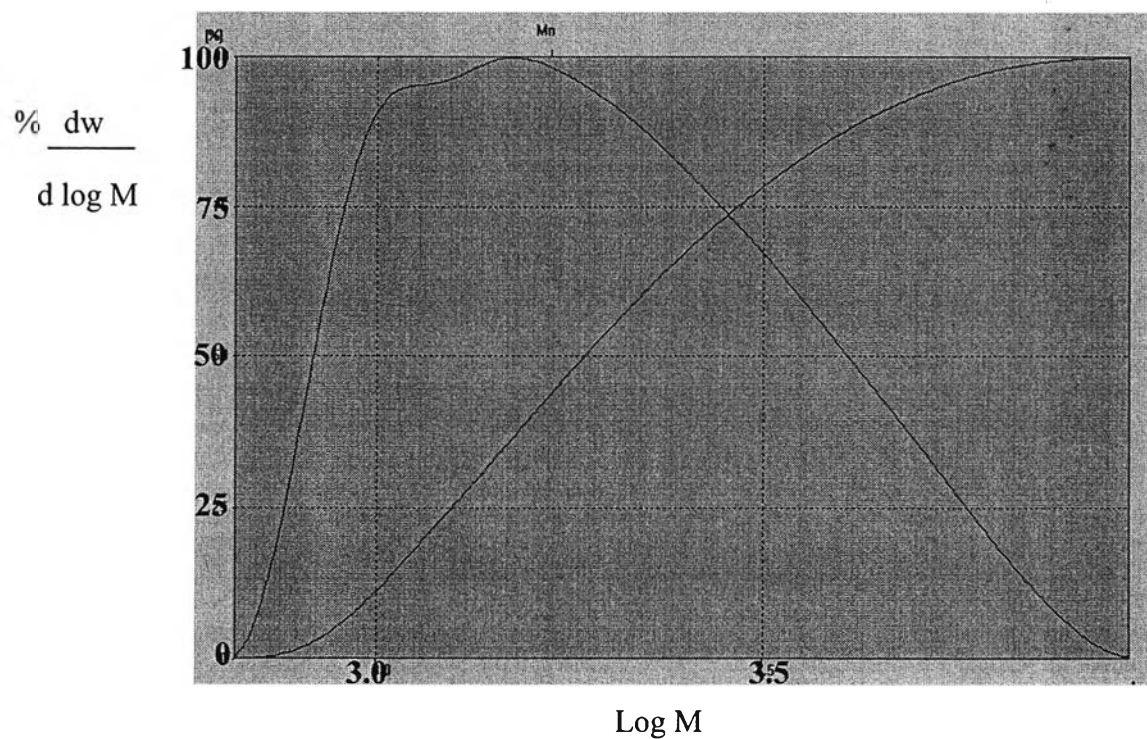
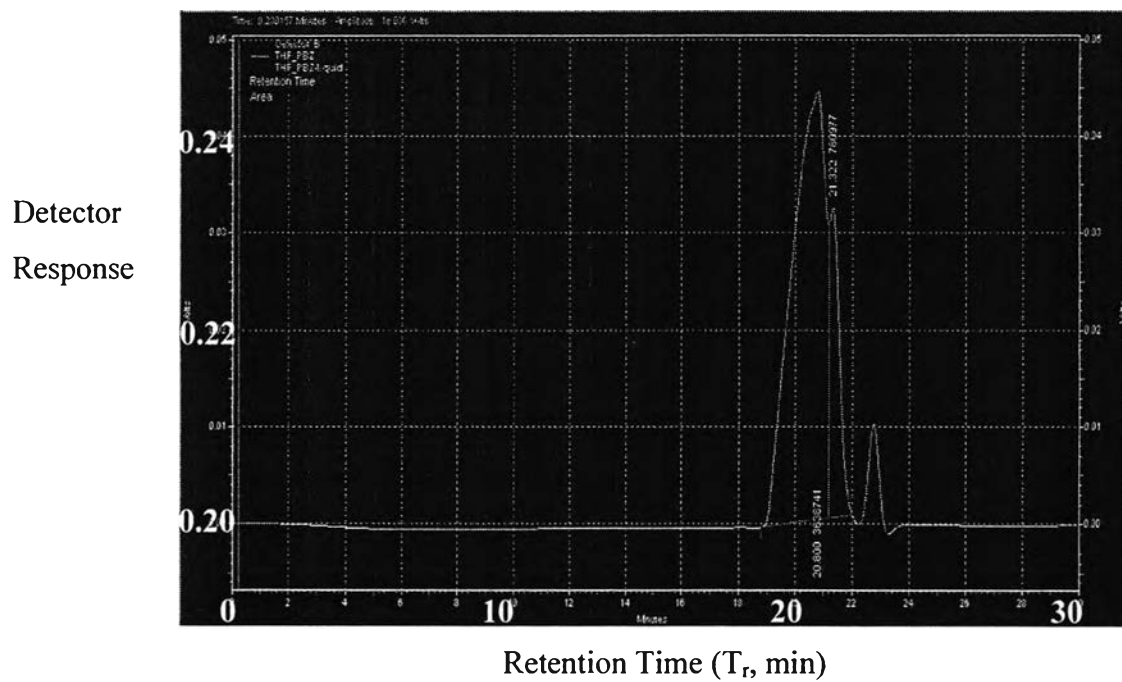


**Figure 4.3** GPC curve for synthesized benzoxazine precursor. With PBZ concentration of 0.5 wt% in THF eluent, Waters Styragel THF Column (7.8\*600 mm), RID-10A detector, 40°C column temperature, 1 ml/min flow rate, and 30 min run time.

Weight average molecular weight ( $M_w$ ) of a precursor was in the range of 2,187–2,278 and number average molecular weight ( $M_n$ ) was 1,637–1,688, showing that its molecular weight was not so high (Takeichi *et al.*, 2005) but it was also not low when comparing with benzoxazine monomers of Sorina-Alexandra *et al.*, 2007. Additionally, it indicated that the structure of precursor contained both of ring-closed structure and ring-opened structure randomly in a polymer chain. It is extremely difficult to remove the ring-opened structure; however this is not a problem because practically both structures will be finally incorporated into the formation of the network.

#### 4.4.1.2 Chemical Analysis of Polybenzoxazine Precursors

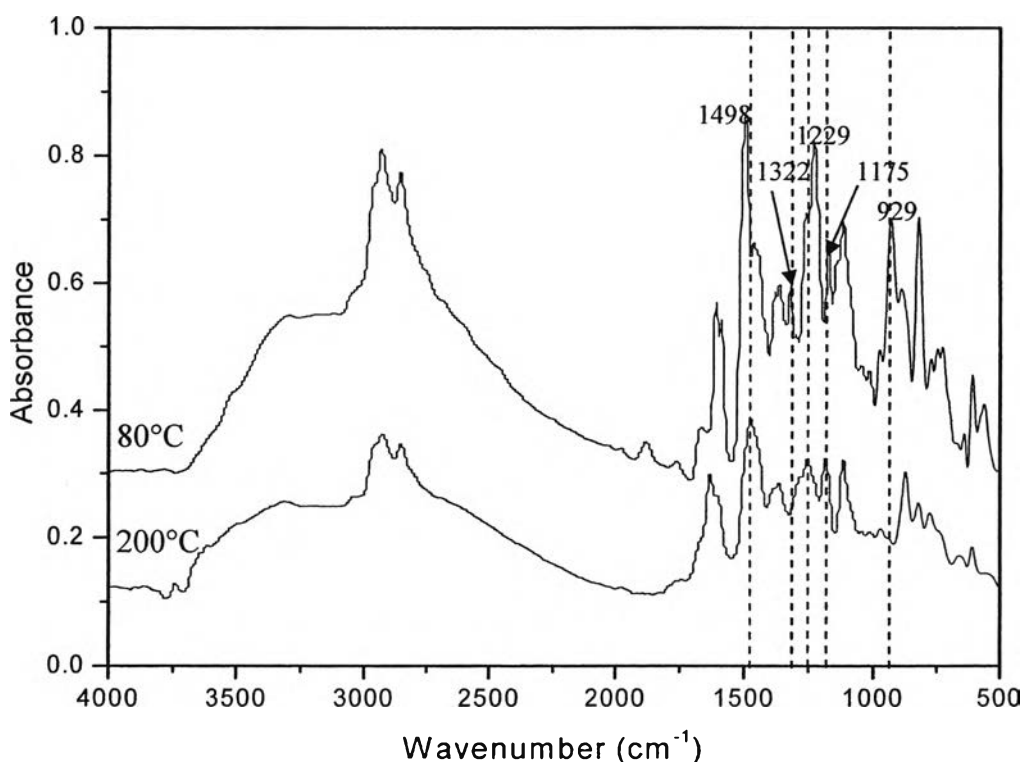


**Figure 4.4** FTIR spectra of uncured (80°C) and cured (200°C) synthesized polybenzoxazine precursors.

The functional groups of the synthesized polybenzoxazine were confirmed by FTIR, as shown in Figure 4.4. The characteristic bands of the benzoxazine

precursor observed at 1229, 1175, and 1322  $\text{cm}^{-1}$ , corresponding to the asymmetric stretching of the C–O–C group, the asymmetric stretching of the C–N–C, and  $\text{CH}_2$  wagging, respectively. Additionally, trisubstituted benzene rings at 1498  $\text{cm}^{-1}$  and out-of-plane bending vibrations of C–H at 929  $\text{cm}^{-1}$  were observed.

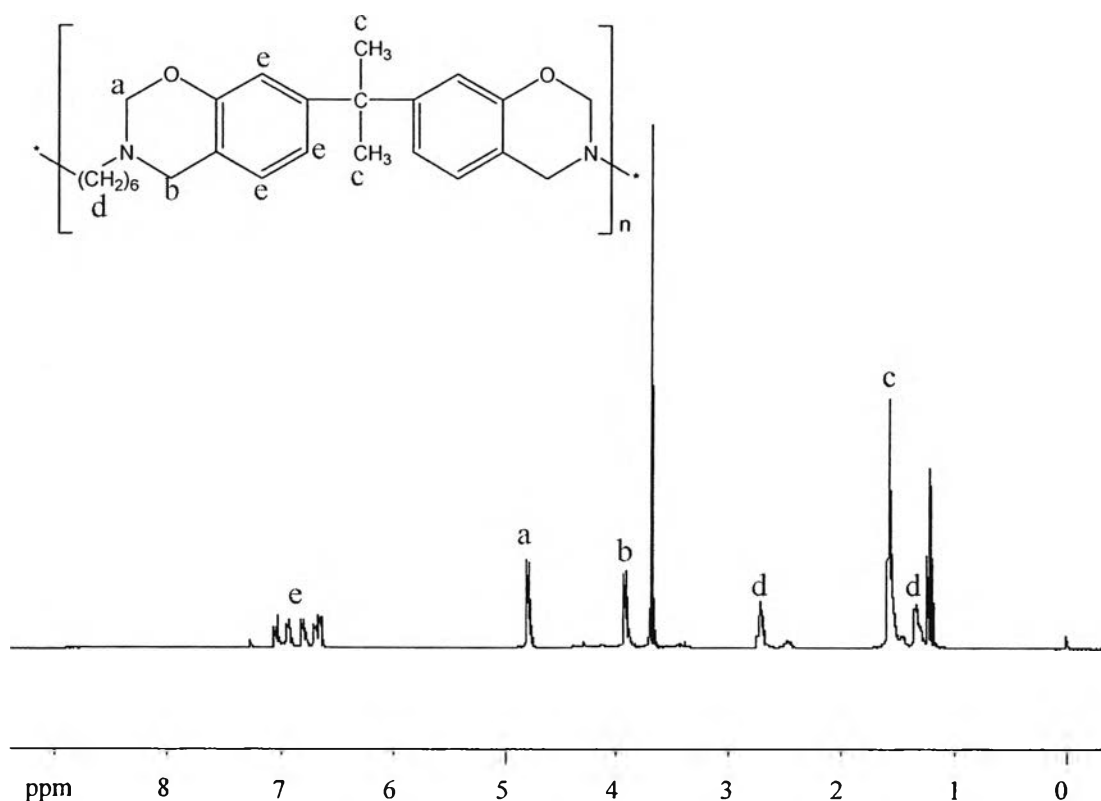


**Figure 4.5**  $^1\text{H}$  NMR spectra of synthesized polybenzoxazine precursors.

The  $^1\text{H}$  NMR spectrum proved that polybenzoxazine had been successfully synthesized (see Figure 4.5). The characteristic peaks of polybenzoxazine were at 4.80 and 3.91 ppm, belonging to methylene ( $\text{O}-\text{CH}_2-\text{N}$ ) and methylene of oxazine ring ( $\text{Ar}-\text{CH}_2-\text{N}$ ), respectively. Also, the methyl proton of bisphenol-A appeared at 1.58 ppm while the methylene protons of 1,6-diaminohexane were observed at 2.72 and 1.34 ppm. The aromatic protons appeared at 6.63–7.05 ppm (Allen *et al.*, 2006).

It could be concluded that polybenzoxazine can be prepared from bisphenol-A, paraformaldehyde, and 1,6-diaminohexane via a quasi-solventless approach, which is similar to that of Takeichi *et al.* (2005) but for our work, less time (~ 3 h) was needed to reach a comparable yield (88%).

#### 4.4.1.3 *Thermal Analysis of Polybenzoxazine Precursors*

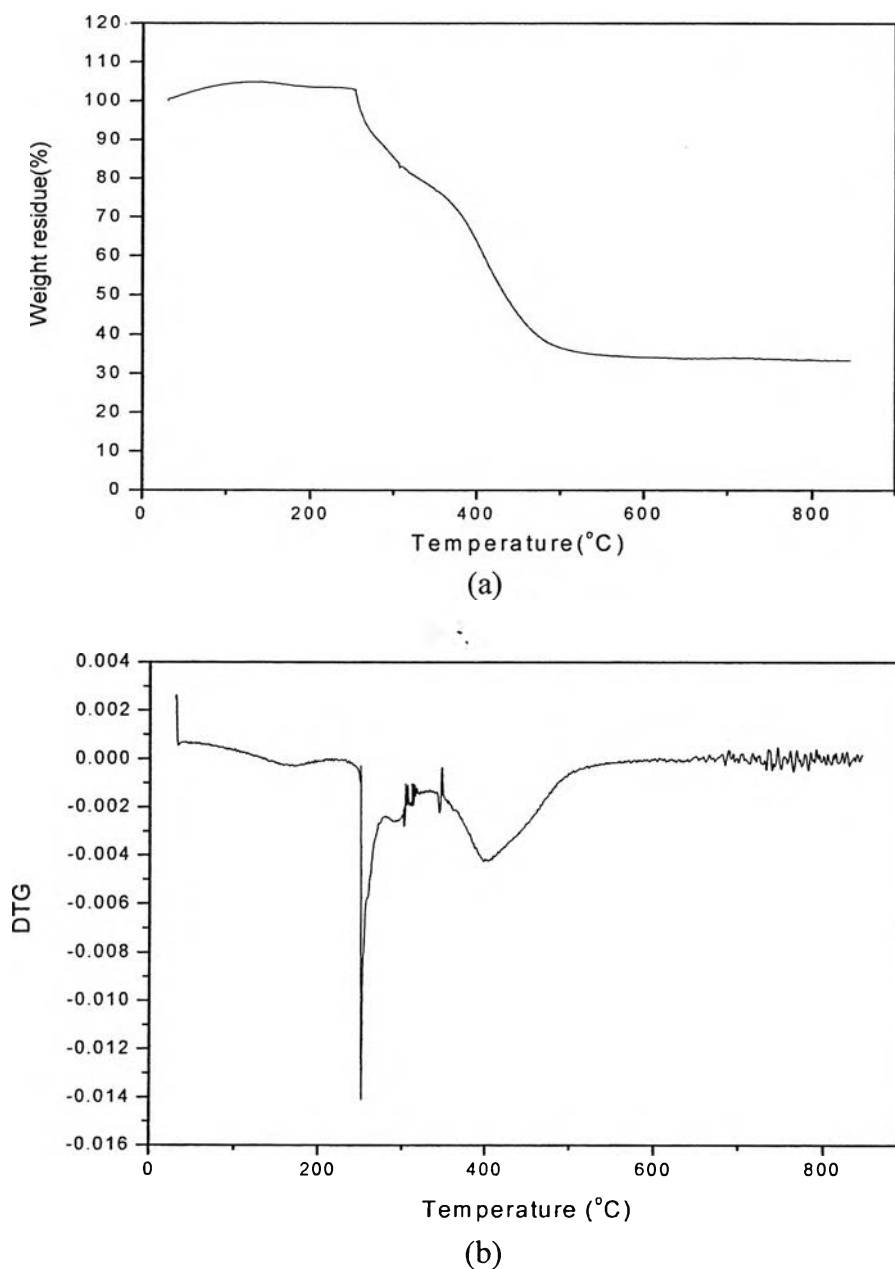


**Figure 4.6** TG-DTA plots of the synthesized polybenzoxazine precursors: (a) weight losses of the sample and (b) differential weight loss curve.

The thermal stability of the polybenzoxazine was investigated by TGA, as shown in Figure 4.6. The decomposition temperature of a precursor was 204°C, which was lower than Takeichi *et al.* reported, and the char residue was about 18 wt% closed to 18.5% of Ishida *et al.*

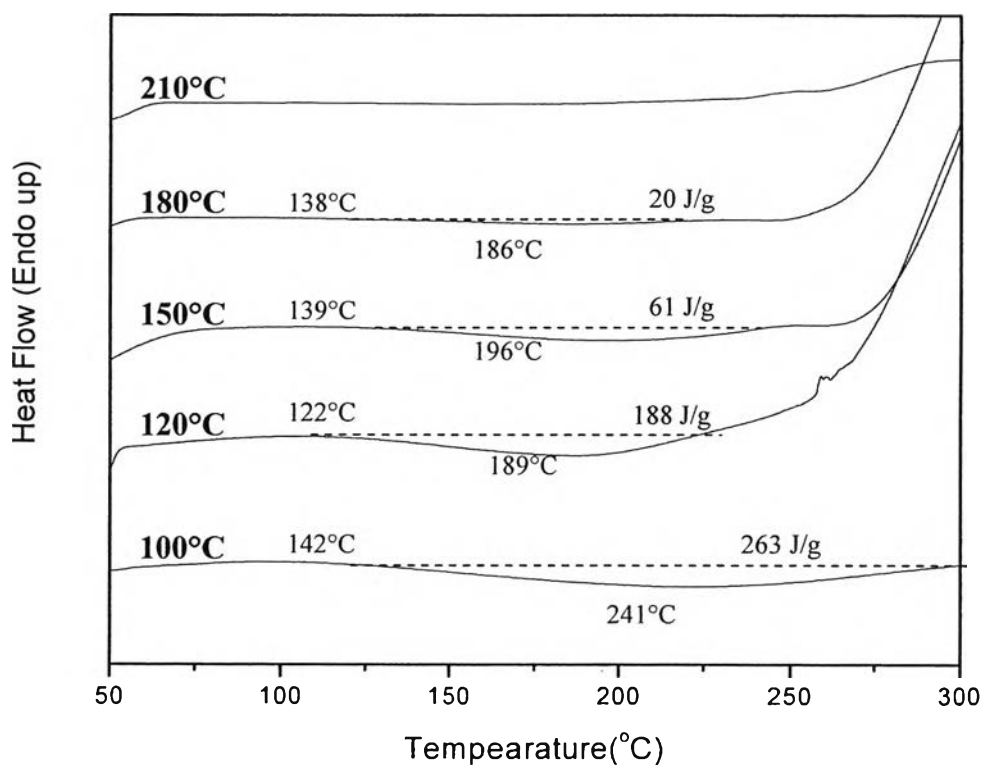


**Figure 4.7** The DSC curves of the synthesized polybenzoxazine precursors after each curing stages.

The DSC profile of the precursor prepared by a compression molding technique; and the values of onset temperature and %conversion after each curing stages polybenzoxazine composites is shown in Figure 4.7 and Table 4.1, respectively. The exothermic onset temperature was at 142°C, corresponding to ring-opening for benzoxazine monomers.

**Table 4.1** The onset temperature and enthalpy of each stages curing polybenzoxazine precursors

Curing temp(°C)	Curing temp(°C)		$\Delta H$ (J/g) of PBZ	% Conversion <sup>a</sup>
	Onset	Peak		
100	142.4	241.5	263	100
120	122.5	189.4	188	72
150	139.5	196.2	61	23
180	138.4	186.1	20	8
210	-	-	0	0

$$^a\% \text{ Conversion} = (\Delta H * 100) / 263$$

The progress of ring-opening polymerization of the precursors was monitored by DSC and FTIR. IR spectra in Figure 4.4 show the decreasing characteristic absorption bands due to the opening cyclic benzoxazines, at 1229  $\text{cm}^{-1}$  (asymmetric stretching of C–O–C of oxazine), at 1175  $\text{cm}^{-1}$  (asymmetric stretching of C–N–C), at 1322  $\text{cm}^{-1}$  ( $\text{CH}_2$  wagging), at 1498  $\text{cm}^{-1}$  (stretching of trisubstituted benzene ring) and at 929  $\text{cm}^{-1}$  (out of plane bending vibrations of C–H). By the end of 200°C cure, which the characteristic absorptions bands for benzoxazine disappeared, suggesting the completion of the ring-opening polymerization. Meanwhile, the DSC thermogram of polybenzoxazine showed that the size of the exotherms decreased with the increasing curing temperature (see Figure 4.7). Also, the exothermic peak completely disappeared after 210°C, which means that the ring opening of oxazine ring was completed.

## 4.4.2 Preparation of Polybenzoxazine–Marl Composites

### 4.4.2.1 Characterization of Marl

Chemical composition of marl was determined by EDX analysis, on the surface of marl particles for at least five points and the results are shown in Table 4.2, on weight and atomic percent basis. It should be noted that Ca, Al, Si, Fe, Mg, and S exist in oxide forms in marl, which made the highest percentage of oxygen elements and the carbon content does not showed in this table due to the overload percentage from tape used in SEM stubs.

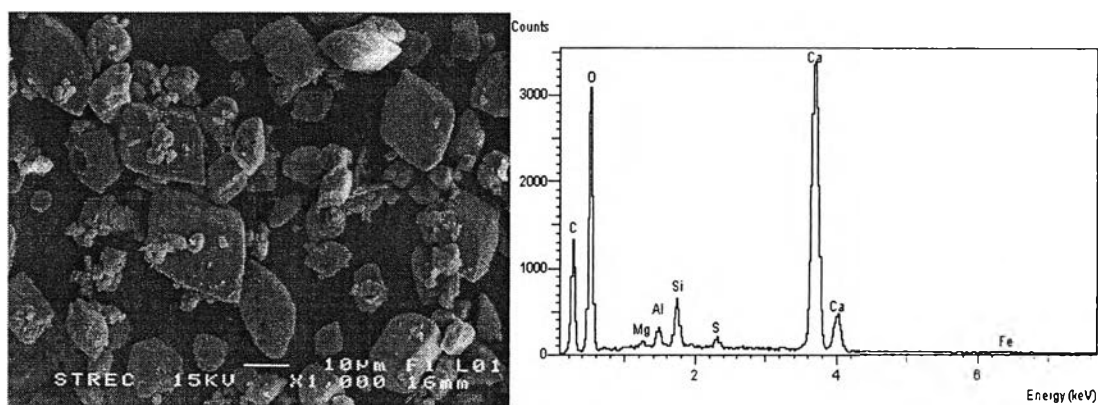


Figure 4.8 SEM-EDX elemental analysis of marl particles.

Table 4.2 Elemental Analysis of marl

Element	Wt%	Atomic%
O	74.57	87.31
Ca	21.08	9.85
Si	2.29	1.53
Al	0.95	0.66
S	0.46	0.27
Mg	0.38	0.29
Fe	0.26	0.09
<b>Total</b>	<b>100.00</b>	<b>100.00</b>

Figure 4.8 is 1000x electron micrographs of the surfaces of marl particles. From the micrograph, marl had a cubic-shaped structure that was similar to the crystal shape of  $\text{CaCO}_3$ , which was the main component in marl. The results from EDX analysis showed that calcium had the highest percentage (except oxygen) element in marl. Therefore, the dispersion of the marl filler in the polybenzoxazine precursors was investigated through the dispersion of calcium.

#### 4.4.2.2 *Thermal Analysis of Polybenzoxazine–Marl Composites*

Marl was blended with synthesized polybenzoxazine at various ratios. The DSC thermograms of the heating scans were recorded for 10–50 wt% marl compositions in the polybenzoxazine precursors are shown in Figure 4.9.

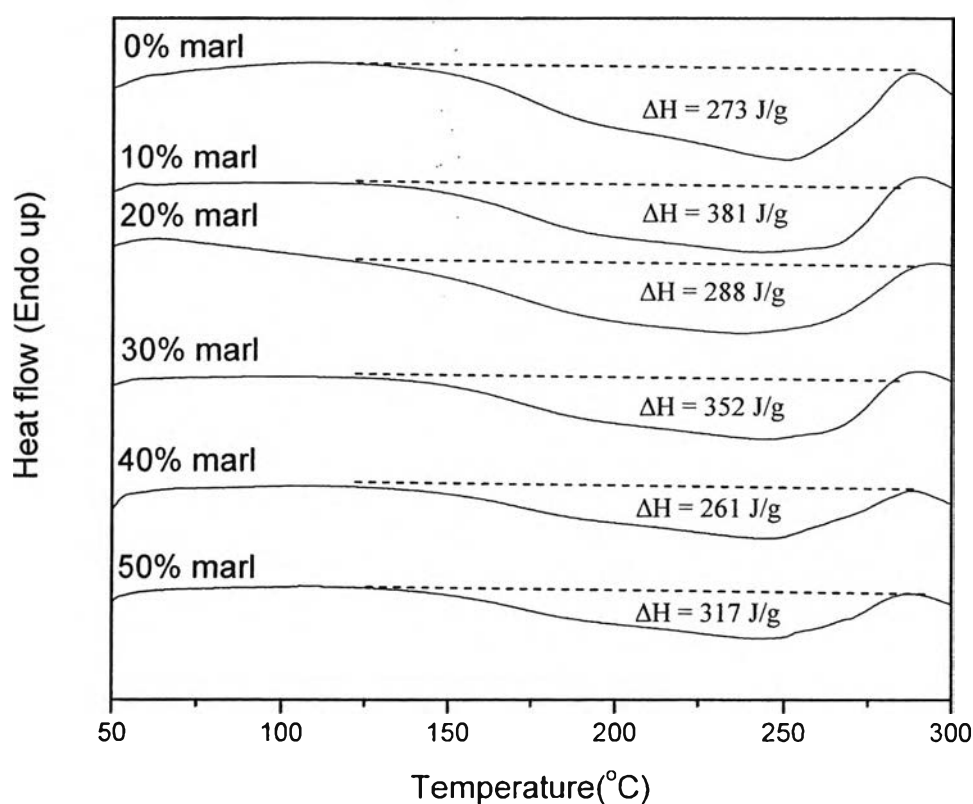


**Figure 4.9** DSC profile of synthesized marl–polybenzoxazine composites (0–50 wt%).

**Table 4.3** Curing temperature and enthalpy of the polybenzoxazine–marl composites after solvent removal by drying in an oven at 80°C for 72 h

% marl in polybenzoxazine	Curing temp(°C)		$\Delta H$ (J/g) of PBZ	% Conversion <sup>a</sup>
	Onset	Peak		
0	153.8	250.8	273	100
10	142.8	244.7	251	125
20	134.9	238.0	230	84
30	144.3	246.5	247	90
40	145.2	245.3	157	57
50	144.7	243.3	159	58

<sup>a</sup>% Conversion =  $(\Delta H * 100) / 273$ ; when  $\Delta H = 273$ , there was no exotherm observed at the second heat of this synthesized PBZ, which meant fully cured PBZ occurred.

Table 4.3 shows that the onset temperatures of the exotherms of the marl–polybenzoxazine composites were not much different from polybenzoxazine. But the exotherm onset of the composites was observed at lower temperature than that of polybenzoxazine. Espinosa *et al.*, 2003 reported that the ring-opening of benzoxazine preferentially react at the ortho positions of free phenolic compounds to form a dimer with a Mannich bridge. They showed the effect of acidity catalyst plays an important role to reduce the curing temperature. Therefore, in this research PBZ–marl composite is believed that the acidic protons such as clay and silica in the marl, were working as acid catalyst, donating proton to the benzoxazine structure and shifting the onset of the ring opening process to lower temperature (Takeichi *et al.*, 2005). It could be preliminarily concluded that marl can reduce the curing temperature of polybenzoxazine precursors.

Additionally, the thermal stability of polybenzoxazine and polybenzoxazine–marl composites was investigated by TGA, as shown in Figure 4.10 and 4.11. Degradation plays an important role in the optimization of curing conditions for the polybenzoxazine. From the TGA results, which are listed in Table 4.4, marl caus-

es an increase in the values of decomposition temperatures and char residue of PBZ. Those values were higher with increasing marl content until the content of 30 wt%, which the decomposition temperature tends to decrease. However the char yield systematically increases with increasing marl content from approximately 28% to 52%. From the derivative weight loss curves, it appeared that each of the marl content degrades in a two-stage weight-loss process. Allen *et al.*, 2006 suggested the degradation mechanism by interpreting infrared spectra of gases evolved during each weight loss stage. They confirmed that the lower temperature weight loss process appears to be associated with the degradation at the Mannich bridge and an associated loss of amine-related compounds. While the maximum of the higher temperature weight loss process is related to the phenol and aliphatic-related compounds.

**Table 4.4** Thermal properties of synthesized polybenzoxazine and polybenzoxazine–marl composites

Samples	$T_d$ onset (°C)		Weight Loss (%)	Char Residue (wt%)
	Peak 1	Peak 2		
Polybenzoxazine	203.7	384.9	81.9	18.1
10% marl–PBZ	220.4	386.8	71.8	28.2
20% marl–PBZ	220.5	387.5	68.8	31.3
30% marl–PBZ	217.3	386.5	61.5	38.5
40% marl–PBZ	215.8	385.4	51.3	48.7
50% marl–PBZ	212.1	382.0	48.5	51.5

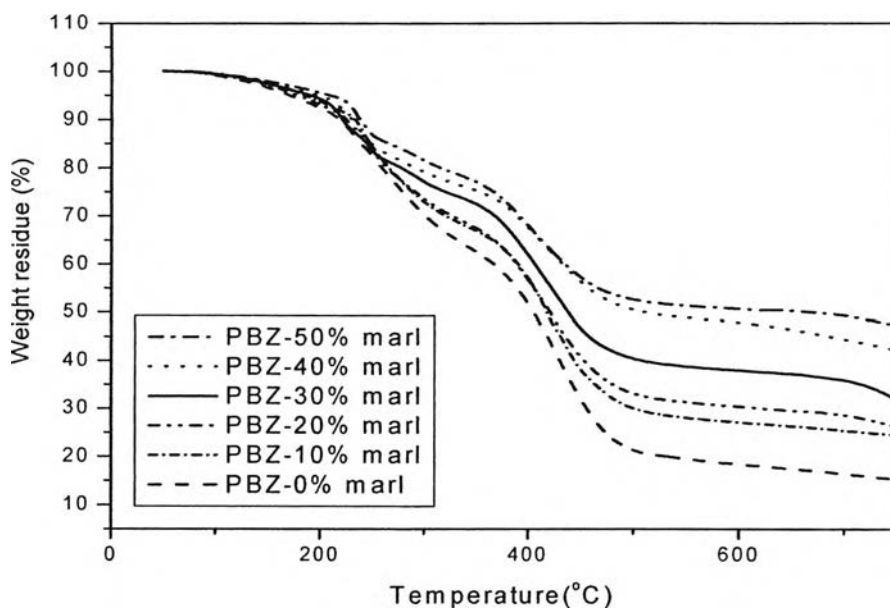


**Figure 4.10** Percent weight loss for the diamine-based of polybenzoxazine-marl composites as a function of marl content as obtained in a nitrogen atmosphere. Percent weight loss of the synthesized polybenzoxazine is also noted for comparison.

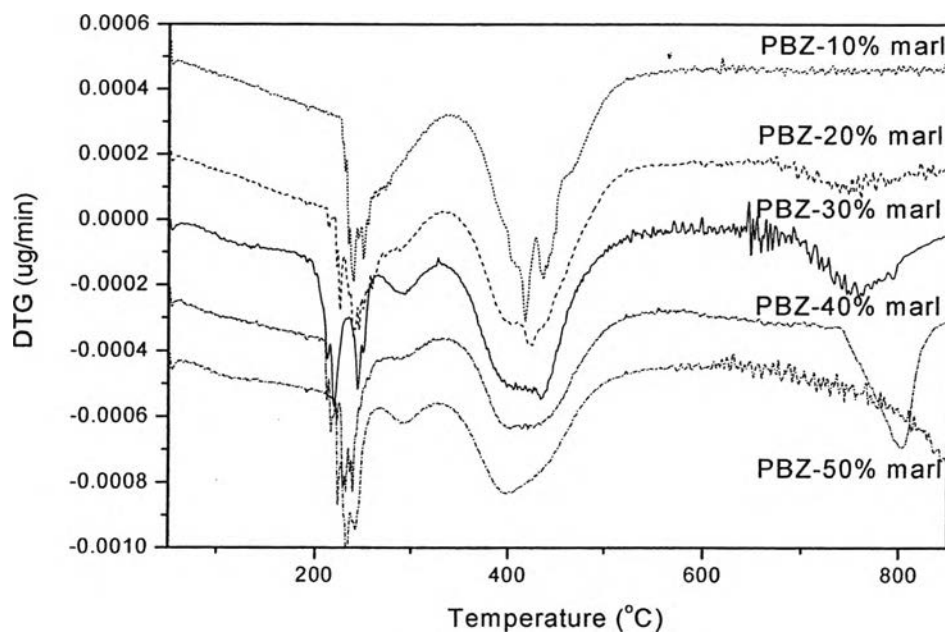


**Figure 4.11** Derivative weight loss for the diamine-based of polybenzoxazine-marl composites as a function of marl content as obtained in a nitrogen atmosphere.

#### 4.4.2.3 *The Morphology of Polybenzoxazine–Marl Composites*

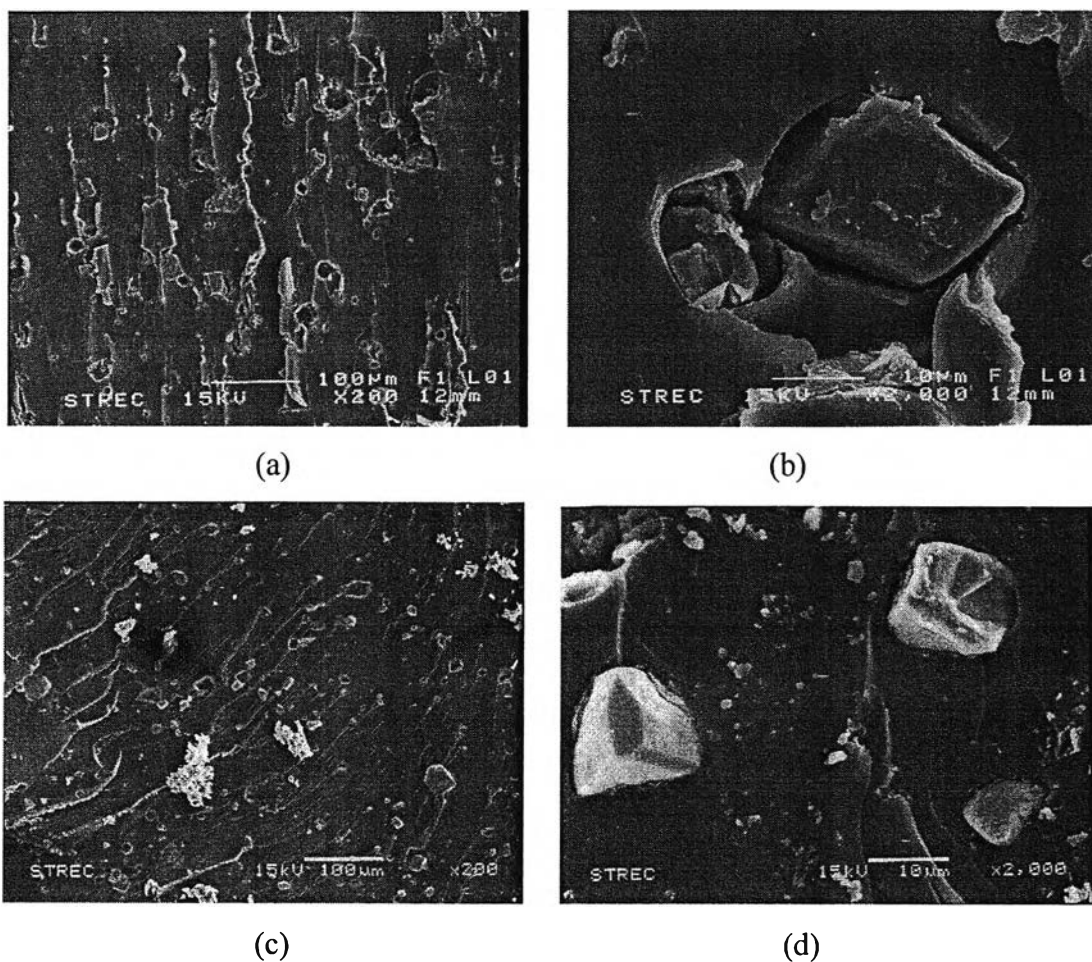


**Figure 4.12** SEM micrographs of the 10% marl–polybenzoxazine composite fracture surfaces (a) 200x, (b) 2000x and the 20% marl–polybenzoxazine composite fracture surfaces (c) 200x, (d) 2000x.

SEM micrographs of the cross section of the fracture surface of the 10 and 20wt% marl–polybenzoxazine composite are shown in Figure 4.12. From the 200x micrographs, the good dispersion of marl filler in polymer matrix was exhibited. And the cubic-shaped structure of marl showed the weak adhesion with the polybenzoxazine precursor, which could be clearly seen in Figure 4.12(b), (d). Weak interfacial adhesion of the polybenzoxazine matrix and the marl filler is probably the reason for the poor mechanical properties. In order to modify the filler–polymer inte-

reaction, stearic acid and amino silane coupling agent, (3-aminopropyl) trimethoxysilane, were used as the surface modifying agents for adjusting the polarity of marl surface. Results of SEM-EDX in Figures 4.13(a) and 4.13(b) show the good dispersion of Ca in polybenzoxazine–marl composites which implied that the filler was well dispersed in the polybenzoxazine matrix without agglomeration of the particles at 30 and slight agglomerates at 50 wt% marl concentrations.

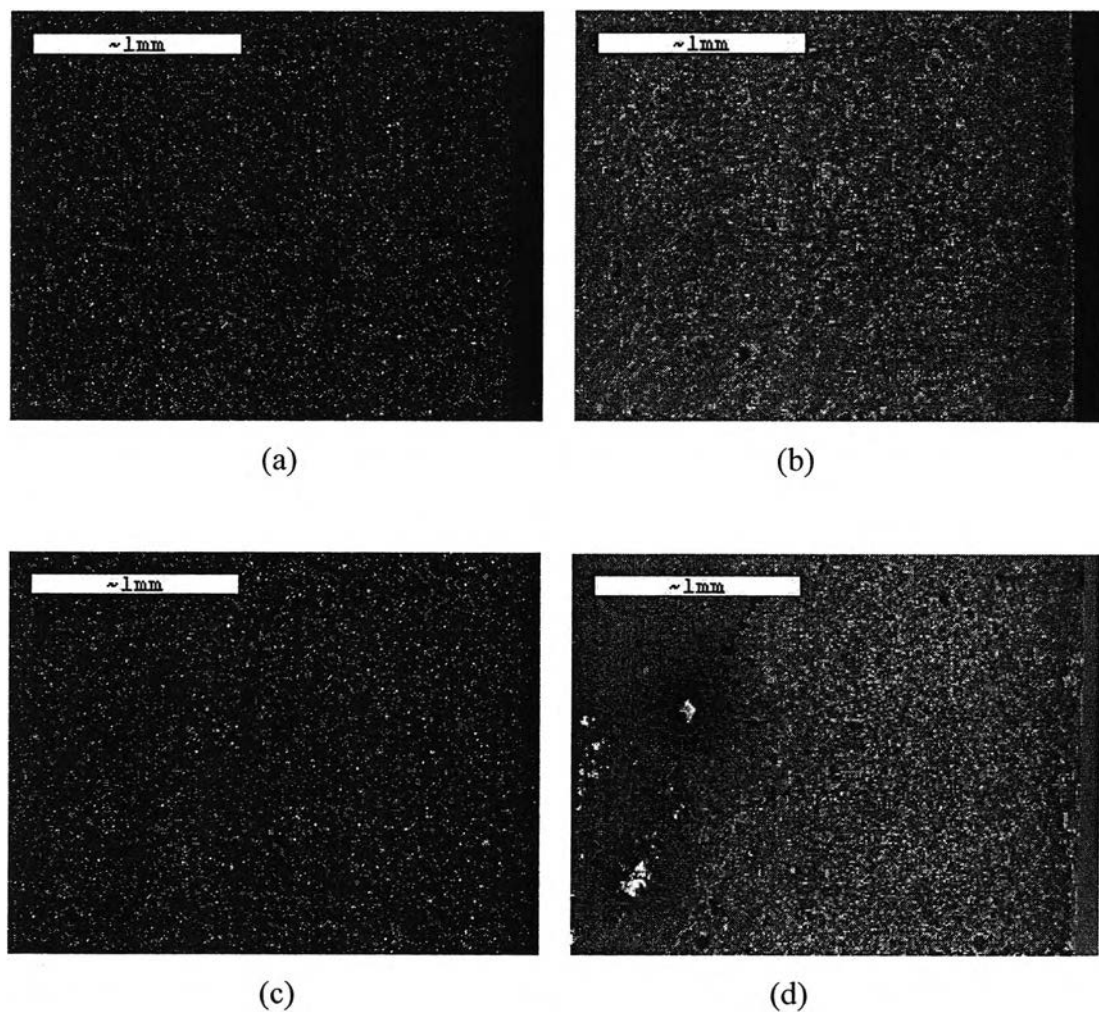


**Figure 4.13** SEM images and their corresponding EDX micrographs of polybenzoxazine–marl composite: (a) 30 wt% marl with Ca mapping, (b) 30 wt% marl SEM image, (c) 50 wt% marl with Ca mapping, and (d) 50 wt% marl SEM image.

#### 4.4.2.4 Surface Modification of a Marl Filler

The weak interfacial adhesion between the surface of the marl and polybenzoxazine as shown by the previous SEM micrographs suggested the necessity for compatibility improvement, by using the coupling agents, i.e. stearic acid and silane coupling agent. The analysis of the chemical structure of the treated marl is shown in Figure 4.14.

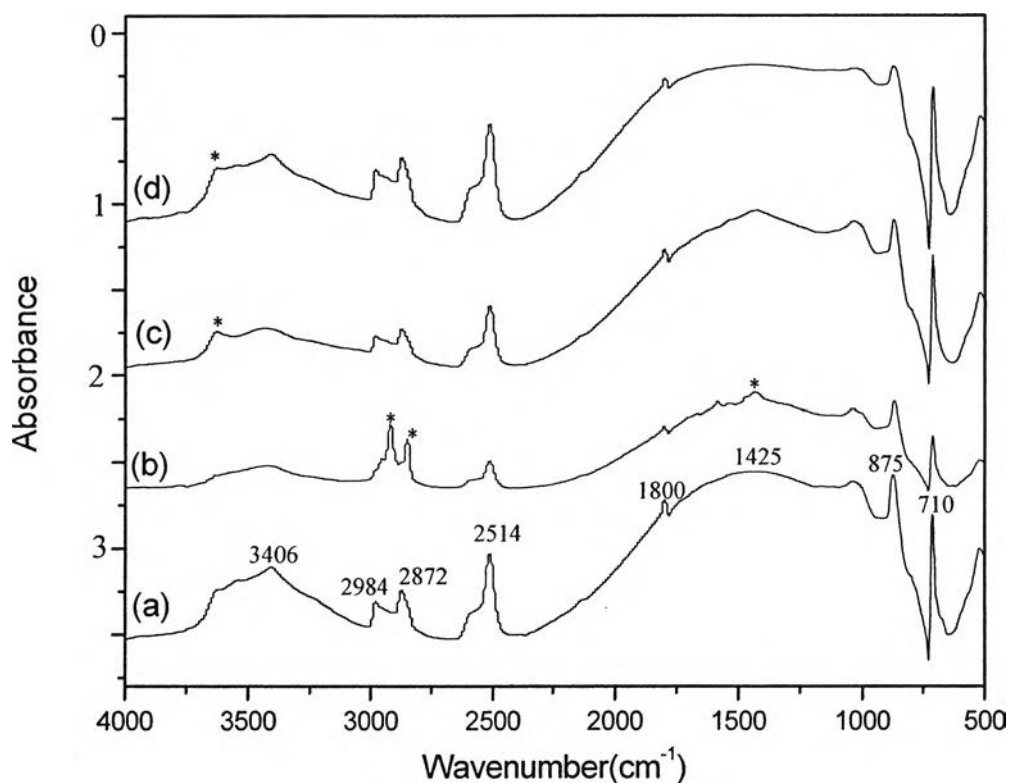


**Figure 4.14** FTIR spectra of marl fillers: (a) untreated marl; (b) stearic acid-treated marl; (c) silane-treated marl; and (d) silane pH 4.5-treated marl.

From Figure 4.14(b), the broad carbonate band (at around  $1500\text{ cm}^{-1}$ ) showed the small part of  $\text{CaCO}_3$  remaining in the system after hydrolysis. The stearic acid treatment shifted the methylene ( $-\text{CH}_2-$ ) stretching peaks ( $2800\text{--}3000\text{ cm}^{-1}$ ) to higher wavenumbers, as proven by Wang *et al.*, 2003. The peaks corresponding to the condensation of the silane coupling agent should be visible at  $1000\text{--}1300\text{ cm}^{-1}$  in Figure 4.14(c) and (d). Although such peaks did not appear clearly, the band at  $3400\text{--}3600$

$\text{cm}^{-1}$  indicated N–H stretching of the silane coupling agent molecule and there were no significantly different peaks, so the pH adjustment is not important for the modification process (Ishida *et al.*, 1998).

From the characteristic bands observed in FTIR spectra, it could be preliminarily concluded that both coupling agents were bounded to the marl by using this method. The thermal and mechanical properties of modified marl–PBZ composites were assumed to improve by these modifications.

#### 4.4.2.5 The Morphology and Thermal Properties of Polybenzoxazine–Modified Surface Marl Composites

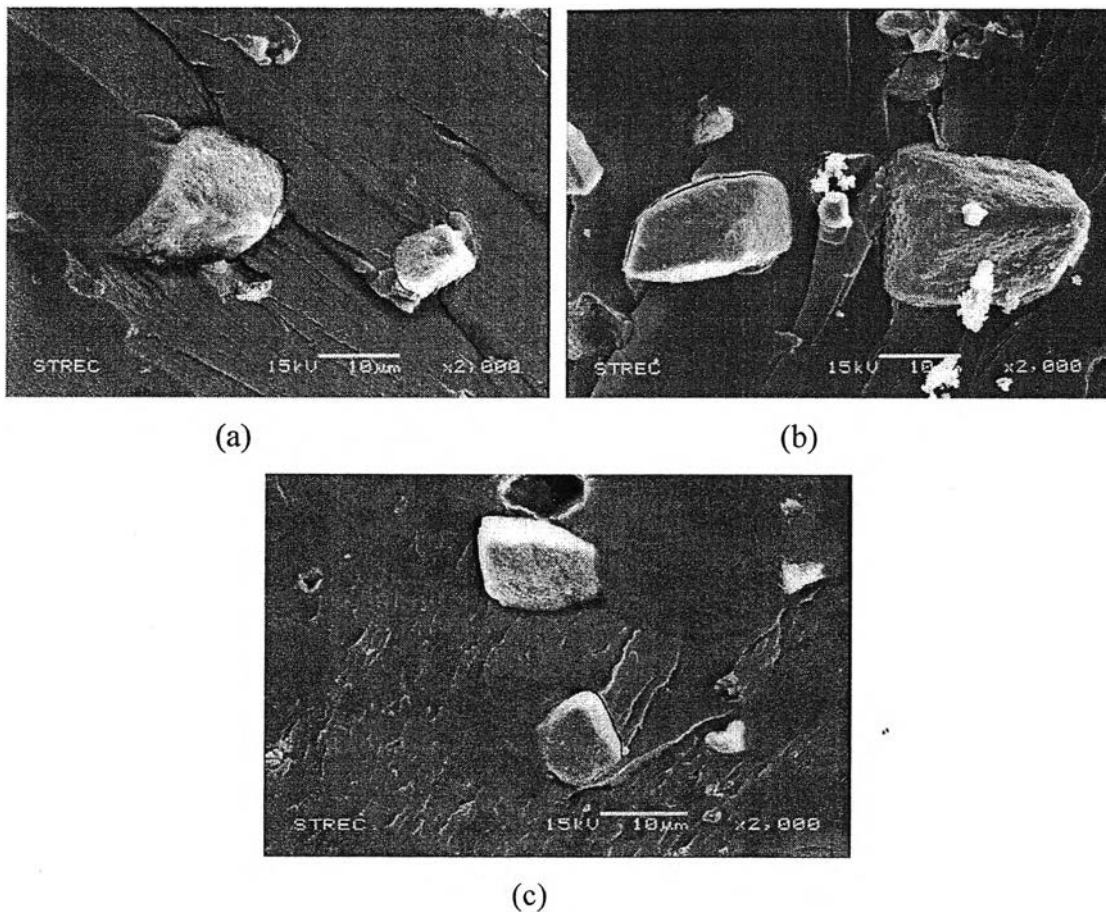


**Figure 4.15** SEM micrographs (2000x) of the fracture surfaces of the polybenzoxazine–marl composites (20 wt%): (a) silane treated, (b) silane pH 4.5 treated, and (c) stearic acid treated.

The morphology of the effect of surface treatment on the interface between PBZ and marl on the surface of the composites were studied by examining the fracture surfaces of the composites by SEM, as shown in Figure 4.15. From Figures 4.15(a–c), it was clearly observed that amino silane-treated and stearic acid-treated fillers (1 wt%) were well embedded in the matrix with matrix coverage around and on the fillers, whereas untreated fillers were not covered with the matrix and there are voids around the fillers. These figures are evidence of the bonding between the coupling agents modified marl surfaces and the polybenzoxazine matrix without the agglomeration of the filler particles. The TGA curves of modified surface marl–polybenzoxazine composites are shown in Figure 4.16, which show the same behavior of polybenzoxazine–marl composite, two-stage weight-loss of the degradation process, and no significantly improve after the surface treatment process.

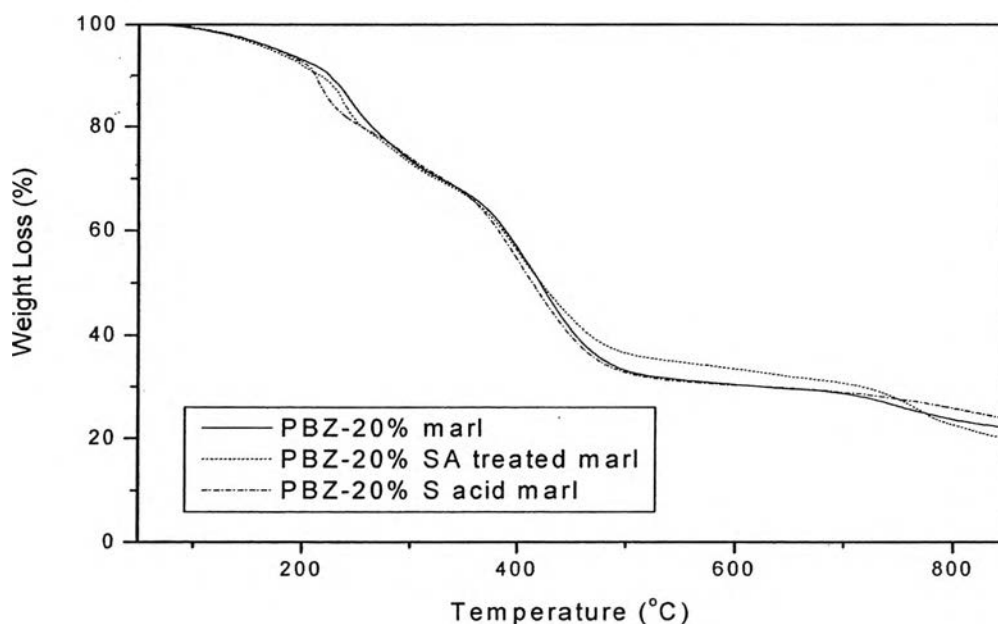


**Figure 4.16** TGA curves of PBZ–20 %wt unmodified and modified marl.

4.4.2.6 *The Mechanical Properties of Unmodified and Modified Surface Marl–Polybenzoxazine Composites*

In this work the mechanical properties were determined by means of flexural properties and impact strength of the linear aliphatic diamine-based of polybenzoxazine, which were tested in accordance with ASTM specifications and are summarized in Table 4.5. The flexural strain, flexural stress, flexural modulus of elasticity, and impact strength are shown in Figures 4.17 to 4.20, respectively.

**Table 4.5** Summary of the flexural properties and impact strength of the polybenzoxazine–marl composites

Marl composition	Flexural testing			Impact strength (kJ/m <sup>2</sup> )
	Strain (%)	Stress (MPa)	Flexural modulus (MPa)	
0%	2.1±0.6	13.4±4.1	527.0±23.4	1.2±0.1
10%	4.5±1.4	14.5±4.4	373.0±69.7	1.6±0.3
20%	6.4±0.9	16.1±1.0	306.7±97.5	2.2±0.2
20%-Silane	4.7±1.8	21.6±5.6	596.4±49.3	2.3±0.1
20%-S acid	4.9±0.2	25.9±0.1	598.6±23.0	2.3±0.2
30%	4.2±0.5	19.9±1.9	596.8±59.0	3.4±0.7
40%	4.5±0.2	27.4±0.6	790.8±14.9	2.0±0.6
50%	2.8±0.9	28.2±6.6	1128.3±59.0	1.3±0.1

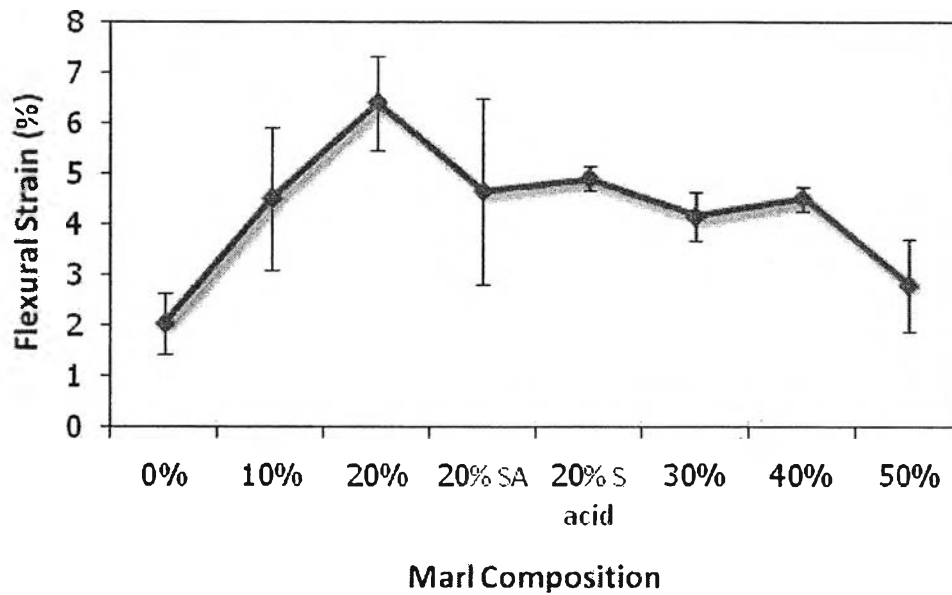


**Figure 4.17** Flexural strain of the synthesized polybenzoxazine-marl composites as a function of marl content as obtained from the 3-point bending experiments. Flexural strain of polybenzoxazine is also noted for comparison.

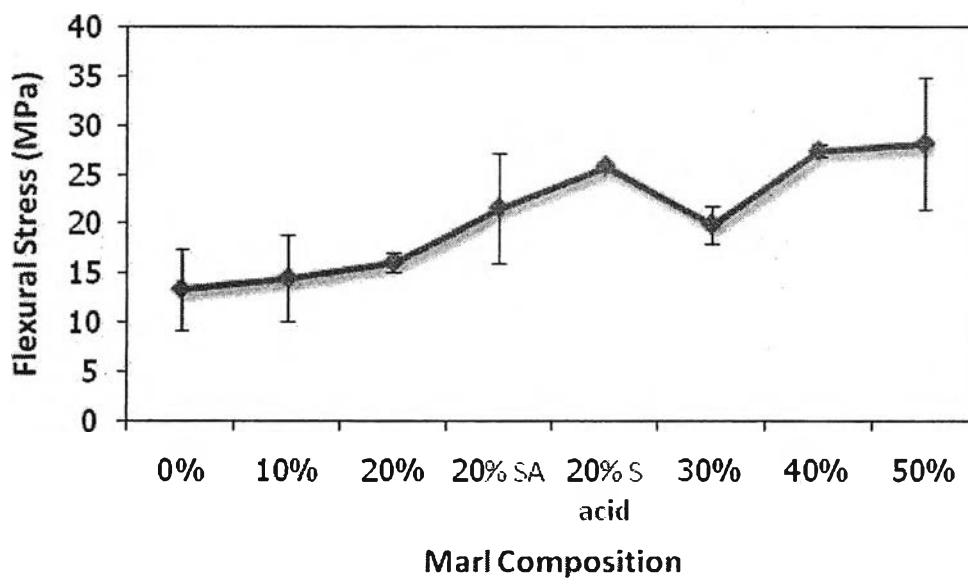


**Figure 4.18** Flexural stress of the synthesized polybenzoxazine-marl composites as a function of marl content as obtained from the 3-point bending experiments. Flexural stress of polybenzoxazine is also noted for comparison.

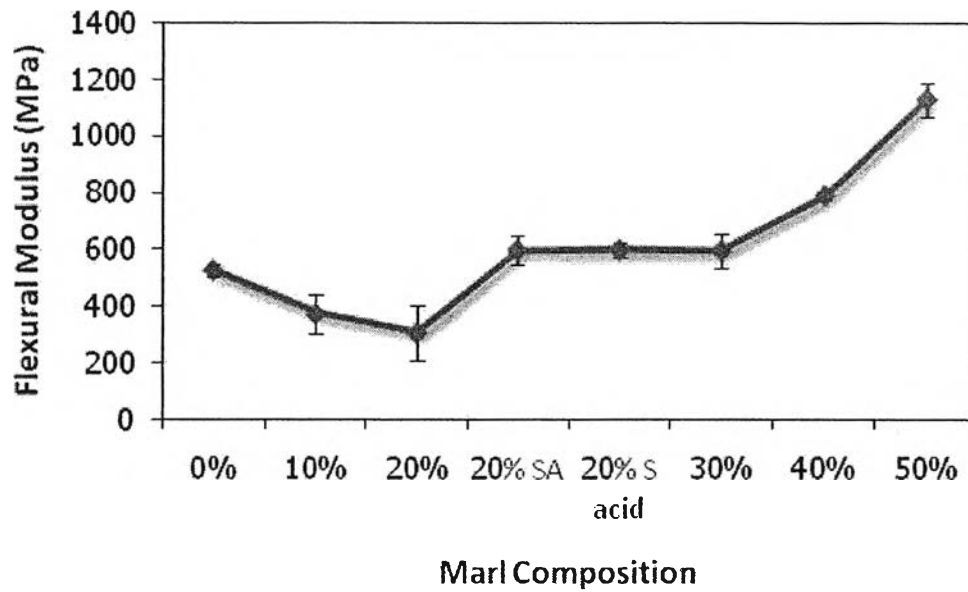


**Figure 4.19** Flexural moduli of the synthesized polybenzoxazine–marl composites as a function of marl content as obtained from the 3-point bending experiments. Flexural modulus of polybenzoxazine is also noted for comparison.

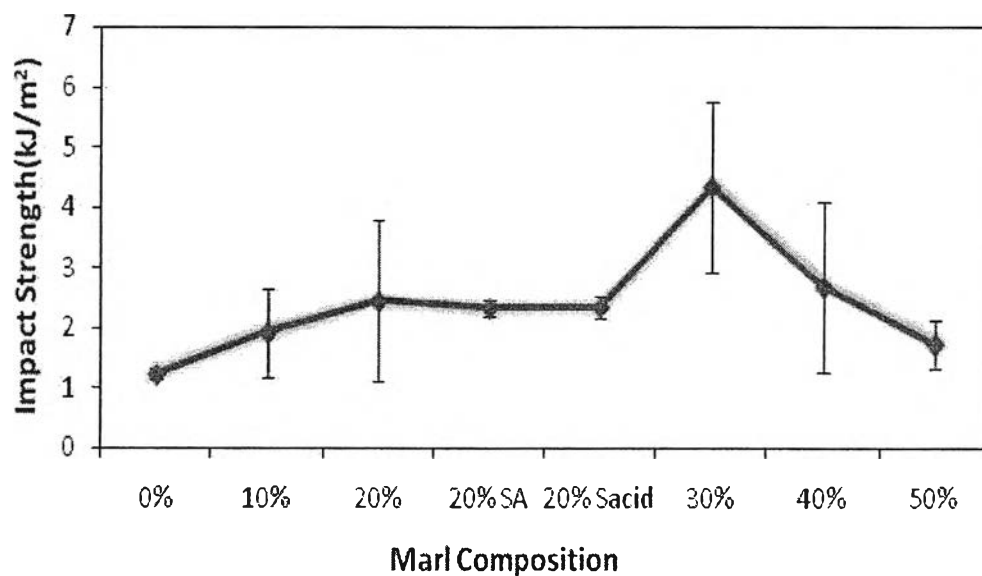


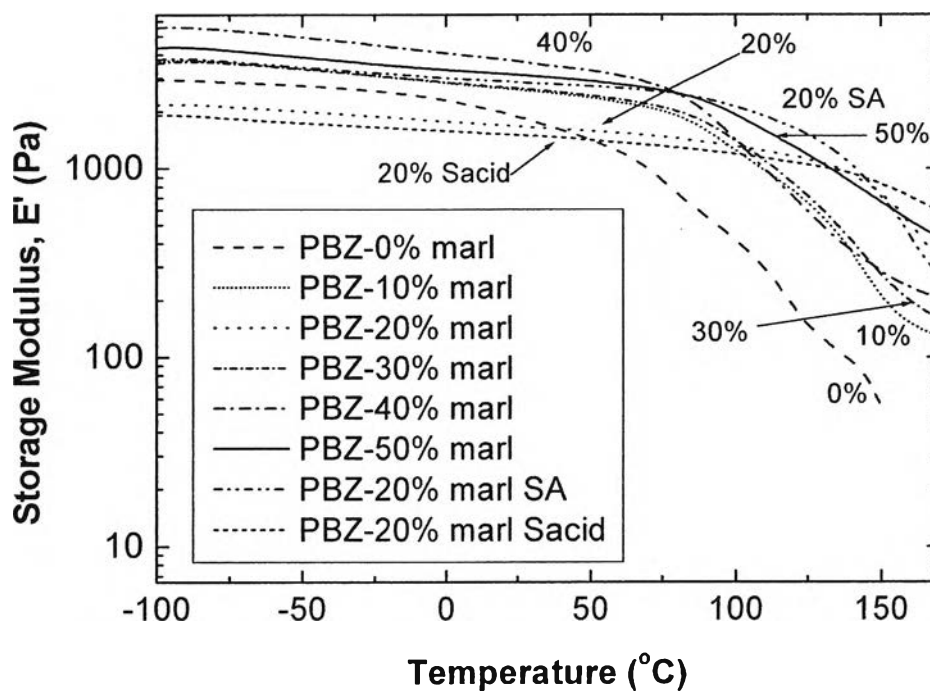
**Figure 4.20** Impact strength of the synthesized polybenzoxazine–marl composites as a function of marl content as obtained from the ZWICK impact testing. Impact strength of polybenzoxazine is also noted for comparison.

Typical polybenzoxazine shows high flexural stress and modulus, but the poor toughness made it easy to break. However in corporation with marl filler, the flexural strain, flexural stress, and elastic modulus of polybenzoxazine–marl composites were much higher than those of pure polybenzoxazine. The flexural strain of polybenzoxazine–marl composites shows a decreasing trend as the filler loading increases. This decrease can be explained by stress concentrations that initiate cracks around filler particles. Whereas the flexural stress of composites tended to increase with an increasing of marl contents because a filler particle can absorb the loaded stress. The elastic modulus of the composite was reduced when adding 10–20 wt% marl and turned to increase with marl loading beyond 20 wt% marl.

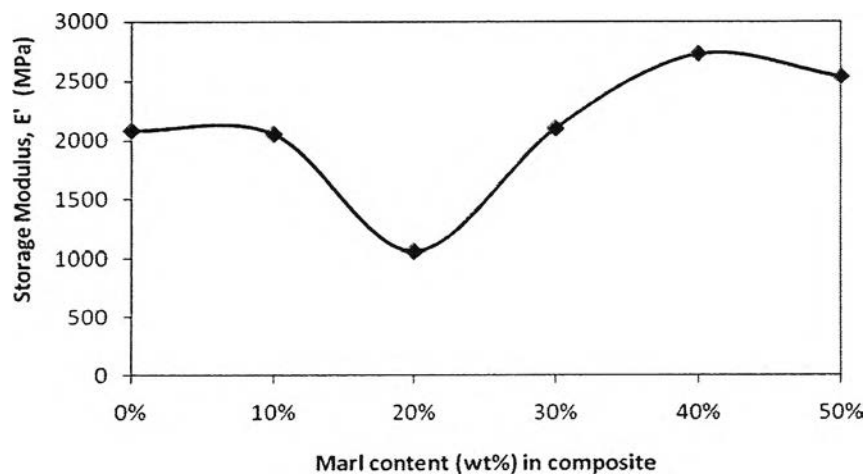
The effect of surface treatment on the mechanical properties was investigated. When comparing at the 20 wt% of marl content in the composite, an increasing in the stress and flexural modulus for the surface modified marl can be explained by better interfacial adhesion between filler and matrix. Without a coupling agent, the only adhesion mechanism is interdiffusion, while the coupling agents lead to hydrogen and covalent bonding between the filler and the polymer matrix (Atikler *et al.*, 2006).

Figure 4.20 shows the influence of surface treatment and filler loading on the impact strength of polybenzoxazine. Impact strength of all composites tended to increase with increasing filler content from 10 to 30 wt% as observed in the Figure. At 20 wt% loading, the increase in impact strength of the composites was 2.2 kJ/m<sup>2</sup> for untreated marl and 2.3 kJ/m<sup>2</sup> for both silane and stearic treated marl. Because of voids, which occurred around the filler revealed by SEM, the untreated fillers were more easily cracked out of the matrix than the treated ones, as shown in an increasing flexural modulus and impact strength after the surface treatment. Both types of surface modifying agent showed the almost same value of improved flexural and impact properties, so it can concluded that amino silane coupling agent and stearic acid make the adhesion between filler and matrix greatly enhanced.

4.4.2.7 *The Dynamic Mechanical Analysis of Unmodified and Modified Surface Marl–Polybenzoxazine Composites*



**Figure 4.21** Storage moduli for the synthesized polybenzoxazine and composites of polybenzoxazine–unmodified surface marl (from 10 to 50 wt% marl contents) and polybenzoxazine–modified surface marl (at 20 wt% marl contents).



**Figure 4.22** Storage modulus at the onset peak of the polybenzoxazine–marl composites as a function of marl contents in the composites.

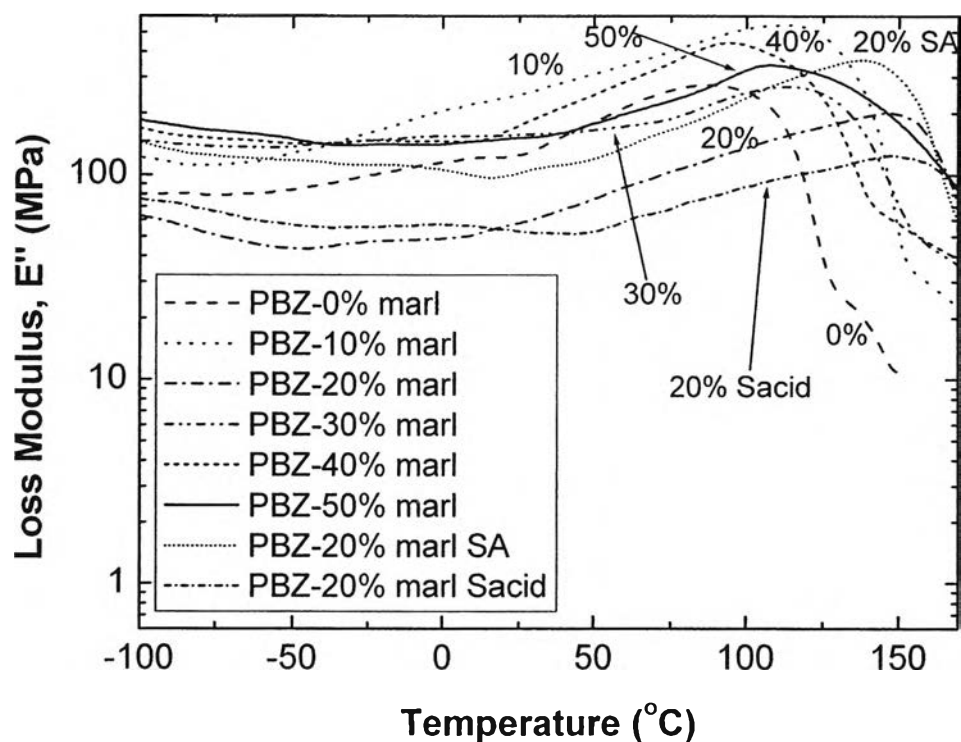


**Figure 4.23** Loss moduli for the synthesized polybenzoxazine and composites of polybenzoxazine–unmodified surface marl (from 10 to 50 wt% marl contents) and polybenzoxazine–modified surface marl (at 20 wt% marl contents).

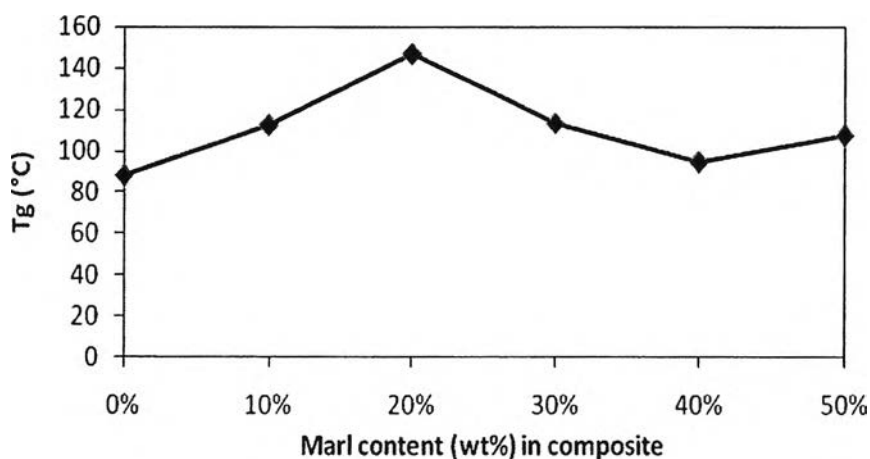


**Figure 4.24** Glass transition temperature of the polybenzoxazine–marl composites as a function of marl contents in the composites.

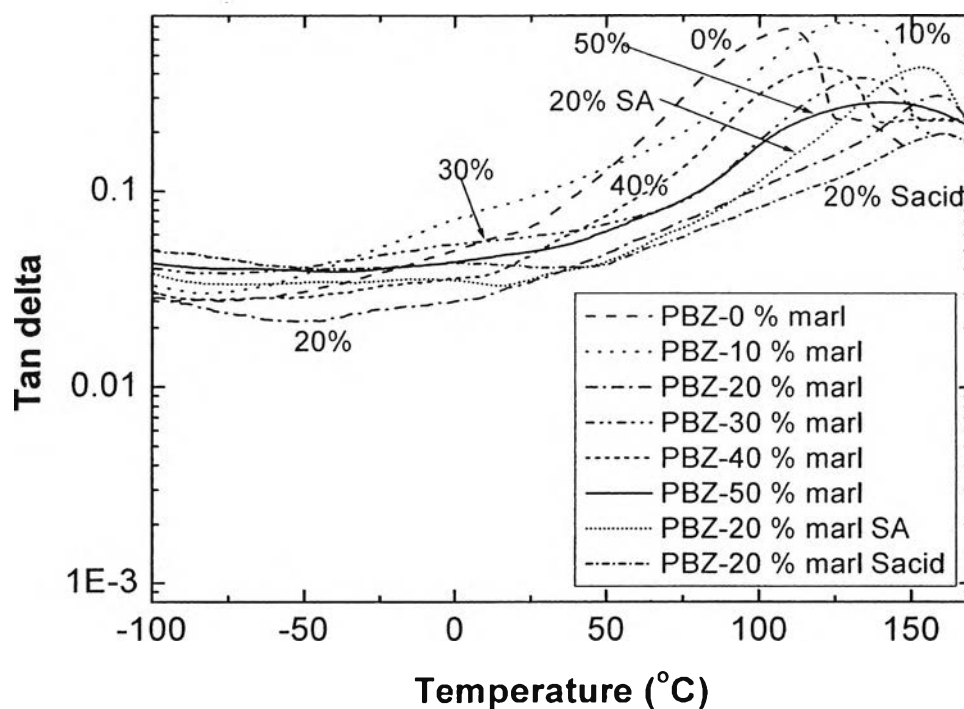


**Figure 4.25** Tan  $\delta$  curves for the synthesized polybenzoxazine and composites of polybenzoxazine–unmodified surface marl (from 10 to 50 wt% marl contents) and polybenzoxazine–modified surface marl (at 20 wt% marl contents).

The dynamic mechanical properties of the synthesized polybenzoxazine and polybenzoxazine–marl composites were measured over the temperature range from  $-100^{\circ}\text{C}$  to beyond the glass transition temperature ( $T_g$ ) of each material. The elastic or storage modulus,  $E'$ , is depicted in Figure 4.21. Contradictory to the trend observed by flexural testing, the modulus was decreased when adding 10–20 wt% marl and turned to increase with marl loading beyond 20 wt% marl, as clearly demonstrated in Figure 4.22. The increasing modulus may come from the more rigidity arising with the higher content of marl filler.

The loss modulus spectrum or viscous component,  $E''$ , for each composite material as the function of temperature is shown in Figure 4.23. The glass transition temperature of the crosslinked material can be determined at the maximum of loss modulus or tan  $\delta$  peaks, and they show the same trend i.e. increase with increasing marl contents from 10–20 wt% and then decrease with more loading. The

opposite trend is observed for storage modulus. These results in Figure 4.24 clearly reveal that the glass transition temperatures of all composites (taken from the maximum peaks of  $E''$ ) are approximately 113, 147, 113, 95, and 107 °C for 10–50 wt% marl contents respectively. These values are significantly higher than that of purely synthesized polybenzoxazine (88°C), indicating that the composites possess lowered chain mobility compared to the neat polybenzoxazine. At the marl content of 20 wt%, the highest  $T_g$  was found and thus showing the highest rigidity. Therefore, it can be concluded that the glass-transition temperature of composites depends on the content of marl filler. This series of polybenzoxazine composites maintain a high stiffness and glass transition temperature.

Additionally, the  $\tan \delta$  values of the composites with different contents of marl filler are shown in the Figure 4.25. These  $\tan \delta$  curves can be used to determine the main  $\alpha$ -relaxation process associated with the glass to rubber transition. For each of the benzoxazine composites,  $\tan \delta$  is located between 100°C and 160°C.

After modification surface of marl by using amino silane coupling agent and stearic acid, the DMA results show that these composites have a higher glass transition temperatures comparing with that of unmodified surface marl at the same content in the composite (20 wt%), which can be verify the improvement of interfacial adhesion between marl and polybenzoxazine matrix.

## 4.5 CONCLUSIONS

In this work, high molecular weight PBZ precursors can be synthesized via a newly developed quasi-solventless method, which could be confirmed by the spectra of FTIR and NMR. Marl filled PBZ composites exhibited lower curing temperature and higher thermal stability than pure PBZ. This was attributed to the acid catalyst effect by marl. The results from SEM revealed the good dispersion of marl in the PBZ, but poor interfacial adhesion arose from the difference in polarity between the marl and the PBZ matrix. The improved interfacial adhesion was achieved by using silane and steric acid coupling agents as investigated by FTIR and SEM. The mechanical properties of marl filled PBZ were poorer than pure PBZ at a low loading but at a high loading of marl (30–50 wt%) flexural strength at yield and modulus of the composites were greatly improved. At 20 wt% marl loading, the flexural modulus of the surface modified marl composites increased significantly over that of untreated marl filled PBZ composites. While the impact strength of composite tended to increase with increasing contents of marl until the loading reached 30 wt% marl, however the impact strength was slightly improved after surface modification on marl surface. In addition, from DMA results, the glass-transition temperature of the polybenzoxazine–marl composite was higher in comparison with pure synthesized PBZ and at 20 wt% of marl content, the modified surface marl showed the higher glass transition temperature.

## 4.6 ACKNOWLEDGEMENTS

The authors would like to thank Mettler Toledo Co., Ltd. for the thermal properties measurement. The authors are grateful for the scholarship provided by the National Excellence Center for Petroleum, Petrochemicals, and Advanced Materials, Thailand. This work is funded by the National Research Council of Thailand (NRCT). The authors would also thank Rachadapisek Sompoch Endowment for Research, Chulalongkorn University for graduate research assistant scholarship.

#### 4.7 REFERENCES

- [1] Agag, T., and Takeichi, T. (2007) High-Molecular-Weight AB-Type Benzoxazine as New Precursors for High-Performance Thermosets. Journal of Polymer Science: Part A: Polymer Chemistry , 46, 1878–1888.
- [2] Allen, D., and Ishida, H. (2006) Physical and Mechanical Properties of Flexible Polybenzoxazine Resins: Effect of Aliphatic Diamine Chain Length Journal of Applied Polymer Science, 101, 2798–2809.
- [3] Altikler, U., Basalp, D., and Tihminlioglu, F. (2006) Mechanical and Morphological Properties of Recycled High-Density Polyethylene, Filled with Calcium Carbonate and Fly Ash. Journal of Applied Polymer Science, 120, 4460-4467.
- [4] Ghosh, N.N., Kiskan, B., and Yagci, Y. (2007) Polybenzoxazines—New high performance thermosetting resins: Synthesis and properties. Prog. Polym. Sci., 32, 1344–1391.
- [5] Huang, J.-M., and Yang S.-J. (2005) Studying the miscibility and thermal behavior of polybenzoxazine/ poly( $\epsilon$ -caprolactone) blends using DSC, DMA, and solid state  $^{13}\text{C}$  NMR spectroscopy. Polymer, 46(19) 8068–8078.
- [6] Ishida, H., and Lee, Y.H. (2001) Synergism observed in polybenzoxazine and poly( $\epsilon$ -caprolactone) blends by dynamic mechanical and thermogravimetric analysis. Polymer, 42(16) 6971–6979.
- [7] Ishida, H., and Lee, H. (2001) Study of hydrogen bonding and thermal properties of polybenzoxazine and poly( $\epsilon$ -caprolactone) blends. Journal of Polymer Science Part B: Polymer Physics, 39(7) 736–749.
- [8] Ishida, H., and Low, H. (1998) Synthesis of Benzoxazine Functional Silane and Adhesion Properties of Glass-Fiber-Reinforced Polybenzoxazine Composites Journal of Applied Polymer Science, 69, 2559–2567.
- [9] Kiskan, B., and Yagci, Y. (2005) Synthesis and characterization of naphthoxazine functional poly( $\epsilon$ -caprolactone). Polymer, 46, 11690–11697.

- [10] Leong, Y., Bakar, M., Ishak, Z., and Ariffin, A. (2005) Effects of Filler Treatments on the Mechanical, Flow, Thermal, and Morphological Properties of Talc and Calcium Carbonate Filled Polypropylene Hybrid Composites Journal of Applied Polymer Science, 98, 413–426.
- [11] Nakatsuka, T., Kawasaki, H., and Itadani, K. (1979) Functional Silane-Modified Calcium Carbonate Journal of Applied Polymer Science, 4, 1985–1995.
- [12] Nichakarn, K., and Magaraphan, R. (2007) High Dielectric Composite Material at Multi-frequency Range. M.S. Thesis. The Petroleum and Petrochemical College. Chulalongkorn.
- [13] Phiriyawirut, P., Magaraphan, R., and Ishida, H. (2001) Preparation and characterization of polybenzoxazine-clay immiscible nanocomposite. Mat Res Innovat, 4, 187–196.
- [14] Sorina-Alexandra, G., Horia, I., Alina, N., and Calin, D. (2007) Thermal Polymerization of Benzoxazine Monomers Followed by GPC, FTIR and DETA. Polymer testing, 26, 162-171.
- [15] Su, Y., Chen, W., Ou, K., and Chang, F. (2005) Study of the morphologies and dielectric constants of nanoporous materials derived from benzoxazine-terminate poly( $\epsilon$ -caprolactone)/polybenzoxazine co-polymers. Polymer, 46, 3758–3766.
- [16] Takeichi, T., Takuya, K., and Tarek, A. (2005) Synthesis and thermal cure of high molecular weight polybenzoxazine precursors and the properties of the thermosets. Polymer, 46, 12172–12180.
- [17] Wang, Y.-X., and Ishida, H. (1999) Cationic ring-opening polymerization of benzoxazines. Polymer, 40, 4563–4570.
- [18] Wang, Y., and Lee, W. (2003) Interfacial Interactions in Calcium Carbonate-Polypropylene Composites. 1: Surface Characterization and Treatment of Calcium Carbonate: A Comparative Study Polymer Composites, 24( 1), 119–131.